JOURNAL OF MATERIALS SCIENCE 39 (2004) 2205–2208

Dynamic shrinkage behavior of hydroxyapatite and glass-reinforced hydroxyapatites

G. GEORGIOU, J. C. KNOWLES
Eastman Dental Institute, UCL, 256 Gray's Inn Road, WC1X 8LD, UK
E-mail: j.knowles@eastman.ucl.ac.uk

J. E. BARRALET
Biomaterials Unit, School of Dentistry, Birmingham University, St Chad's Queensway, Birmingham B4 6NN, UK

Hydroxyapatite (HA) has generated a great deal of interest over recent years as a surgical implant material [1]. This is attributed to its bioactive nature which stems from the chemical similarity it has with the inorganic phase of natural bone [2–6]. Biologically, HA can serve as a means by which tissue, such as bone, can regenerate, and can be developed in various forms to serve this purpose either as a scaffold, coating or as a monolithic block [3]. However, mechanically, HA is limited due to its low load bearing capacity [1].

Recent studies have shown that the introduction of phosphate based glasses as a sintering aid is known to reinforce HA mechanically [2]. Furthermore, phosphate glasses are known to facilitate the decomposition of the HA phase to β-tricalcium phosphate (β-TCP) and can also lead to further inversion of the β-TCP phase to α-tricalcium phosphate (α-TCP) [2–5]. These phase changes can be brought about by ionic substitutions between the glass and HA that occur during liquid phase sintering, to which the extent of substitution can depend on the chemical nature of the glass [2, 4]. Some glasses may contain mineral ions such as Na^+ or Mg^{2+} which could be responsible for structural changes in the HA lattice during the sintering process.

Physical considerations must be highlighted to explain the effect these phosphate glasses have on HA. Phosphate glasses, when incorporated into HA, melt at lower temperatures compared with HA and can act to increase densification by enhancing the sintering mechanisms [2, 3, 6]. Although this process is known to improve the material mechanically it was important in this study to emphasize how this may be correlated to changes in density, porosity and in particular, shrinkage.

A glass was produced with a composition of 32 mol% CaO, 23 mol% Na_2O and 45 mol% P_2O_5. The starting reagents used to prepare the glass consisted of $NaHPO_4$, P_2O_5 and $CaCO_3$. These were mixed thoroughly and placed in a platinum crucible, melted at 1000 °C for 1 h, and then poured onto a steel plate and allowed to cool. The resulting glass was then ground to a fine powder using an agate grinder.

The glass (5 or 10 g) powder was placed in a porcelain mill pot and milled dry for 24 h. HA (supplied by Plasma Biotal Ltd. UK) was then added to the mill pot at either 195 or 190 g to give glass additions of 2.5 and 5 wt% glass additions respectively (see Table I). Methanol (300 ml) was also added and the mixture was then wet milled for a further 24 h. The resulting slip was then dried at 70 °C and the dry powder was then sieved to 75 μm.

Four grams of powder were placed into a steel die and uniaxially pressed at 20 tons using a hydraulic press to give 30 mm compacted discs. The discs were fired at a heating rate of 4 °C min^{-1} to 1200, 1250, 1300 and 1350 °C. The specimens were held at the appropriate temperature for 1 h then furnace cooled. The dimensions of the sintered discs were approximately 25 mm in diameter and 2.5 mm in thickness.

The shrinkage behavior of the HA compacts in the various atmospheres was studied using a push rod type dilatometer (Netzch 402E). The shrinkage was measured in the axial direction. The sample support, Netchze measuring unit, and displaceable furnace of the dilatometer were mounted horizontally. The length change measurements were made by a transducer, which was maintained at a constant temperature by means of water circulation from a constant temperature bath. The accuracy of the measurement change in length was within $\pm$0.1 mm. The temperature was measured using a calibrated thermocouple, which was placed directly above the sample. A small force of 0.2 N was applied to the sample through the push rod in order to maintain contact with the sample. The selection of the temperature program was controlled by a computer via a data acquisition system. Correction was applied to the expansion of the system by making a run under identical conditions using a standard sample (Al_2O_3). The shrinkage behavior was monitored from 0 to 1350 °C with a heating rate of 4 °C min^{-1}.

Density measurements were performed on each sintered specimen using the Archimedes principle. The measurements were carried out in distilled water. These were then compared with the theoretical densities calculated from the Rietveld analysis to give the porosity.

Samples taken from the flexure test were ground to a fine powder, placed in a specimen holder and then analyzed on a Philips PW 1780 diffractometer with Ni filtered Cu K_α radiation ($K_{\alpha1}$ = 1.5406 Å, $K_{\alpha2}$ = 1.5444 Å) at 40 kV and 30 mA. The data were collected with a scintillation counter between $10° < 2\theta < 90°$

TABLE I

Specimen	HA addition (g)	Glass addition (g)	Glass addition (wt%)
HA	200	0	0
GR-HA (2.5)	195	5	2.5
GR-HA (5)	190	10	5

with a step size of 0.02 ° and a count time of 12 s using flat plate geometry.

The structure refinement was carried out using General Structure Analysis Software (GSAS, Los Alamos National Laboratory). A standard model for each of the three phases was used for the refinement of the samples and they were determined from the Daresbury Crystal Structure Database. The HA model was based on the single crystal structure determination with P63/m space group, the β-TCP second phase was based on the R3CH model and the α-TCP phase was based on the P21/ a model.

The software calculates the phase weight percentage (P) and the theoretical density (ρ) (assuming no porosity) of each phase present in the specimen. The calculation for these numbers does not include any error determination. From these, the overall theoretical density of the sample can be determined:

$$(P_{\mathrm{HA}} \times \rho_{\mathrm{HA}}) + (P_{\beta\text{-TCP}} \times \rho_{\beta\text{-TCP}}) + (P_{\alpha\text{-TCP}} \times \rho_{\alpha\text{-TCP}}) = \text{Overall theoretical density}$$

From the data for the measured density and the overall theoretical density, the porosity is calculated using:

$$[1 - (\text{Recorded density}/\text{Theoretical density})] \times 100(\%)$$

This again does not have an associated error with it.

Mechanical testing used the biaxial flexure strength test method with a concentric ring testing jig with a loading ring of 10 mm and outer supporting ring of 20 mm. Ten specimens were tested to failure for each of the firing temperatures on an Instron machine at a crosshead speed of 5 mm min^{-1}. The biaxial flexure strength was determined from the load displacement behavior.

Fig. 1 shows the shrinkage of HA and GR-HA specimens as a function of temperature. At approximately 900 °C HA starts to undergo shrinkage, with both GR-HA's undergoing shrinkage at approximately 1000 °C. It is evident that shrinkage for HA occurs at lower temperatures compared to the GR-HA samples. At approximately 1300 °C the rate of shrinkage starts to decrease for all specimens. However, at the final temperature, 1350 °C, there are distinct differences in the total shrinkage, with the HA specimen displaying the greatest shrinkage.

Shrinkage is governed by the rate of densification (Fig. 2) and through reduction in porosity (Fig. 3). It is therefore important to mention any correlation between porosity and shrinkage and also if additional factors such as secondary phases correlate with changes observed for shrinkage.

The differences in the values between 1200 and 1350 °C may be attributed to phase transformation (Figs 1 and 4). Both GR-HA materials contain a fraction of β-TCP and α-TCP secondary phases at all four temperatures. Decomposition of HA to β-TCP and subsequent inversion to α-TCP introduces an increase in unit cell volume which may explain why the GR-HA materials undergo less shrinkage. This also applies to differences in the level of shrinkage between the GR-HA materials at 1300 and 1350 °C, since GR-HA (5) contains a higher amount of the α-TCP phase (α-TCP—has the largest unit cell volume) at these temperatures. The differences seen in porosity at the same temperatures (Fig. 3) show some correlation with the level of shrinkage. GR-HA (5) exhibits a minimal increase in porosity at 1300 and 1350 °C and mirrors the differences seen in the shrinkage between the GR-HA materials. However,

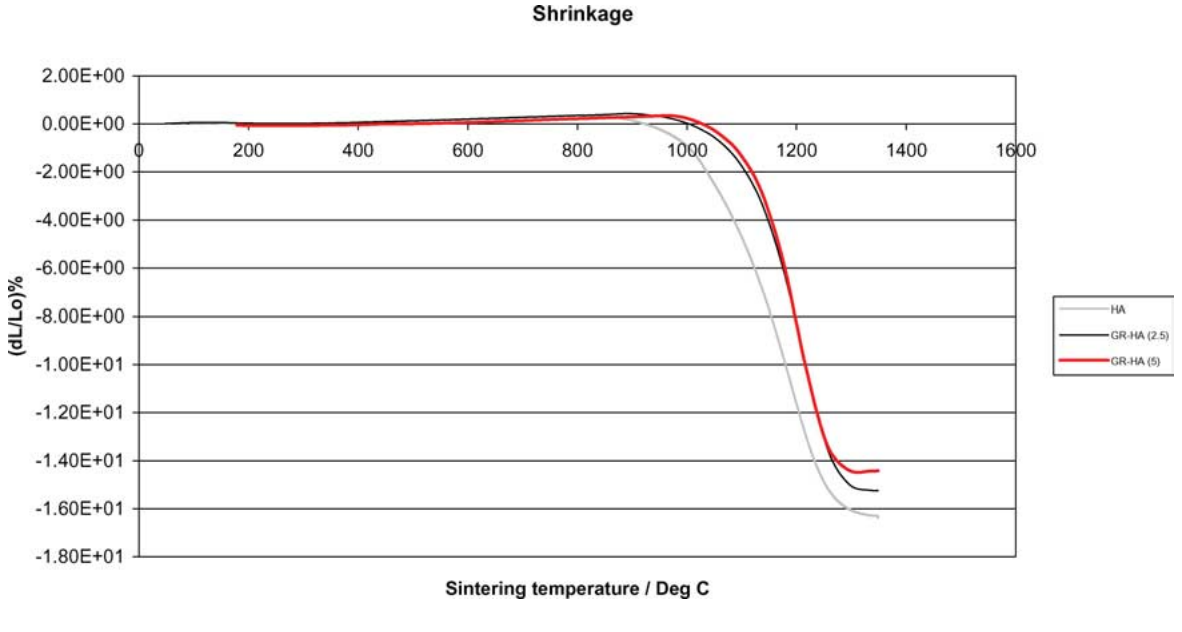

Figure 1 Shrinkage of HA and GR-HA as a function of temperature.

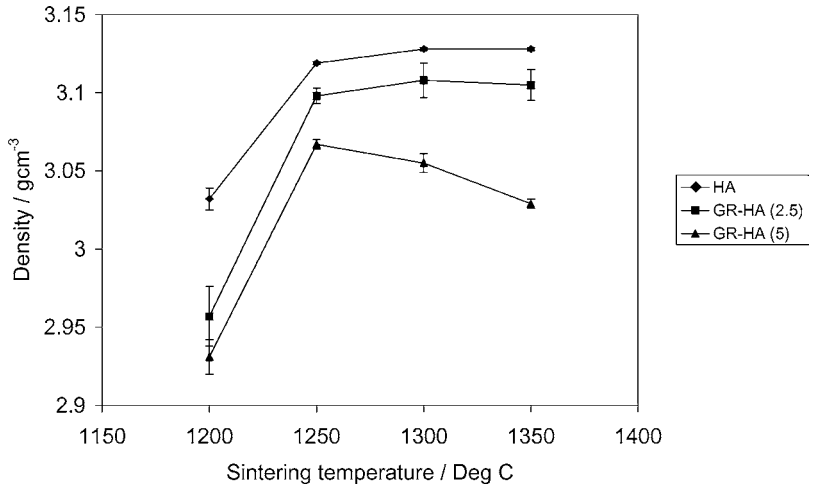

Figure 2 Effect of firing temperature and glass addition on density.

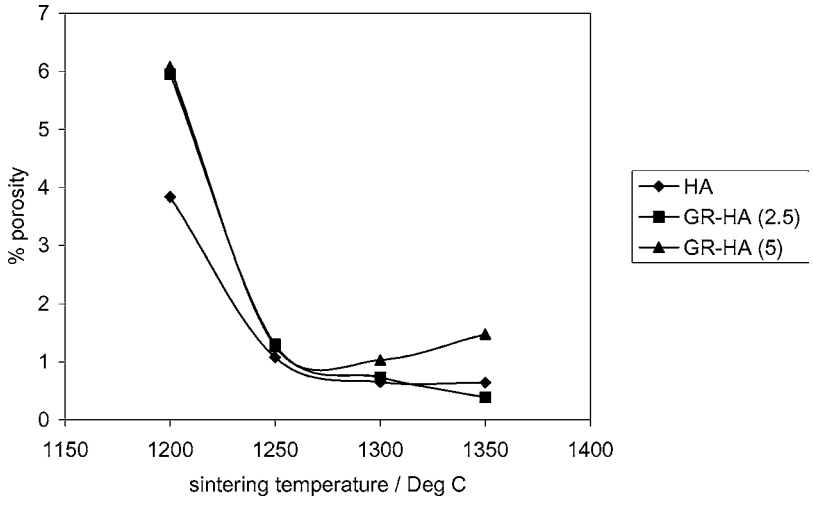

Figure 3 The effect of glass addition and firing temperature on porosity.

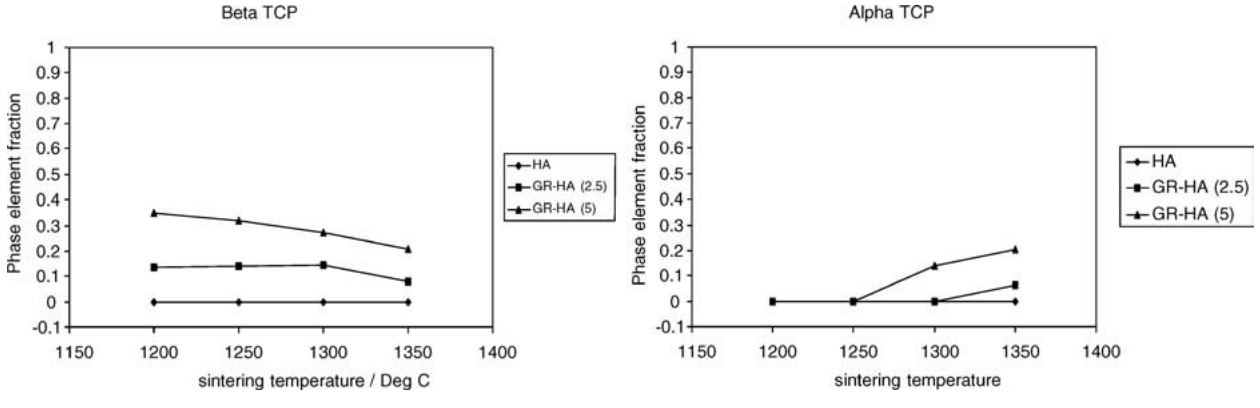

Figure 4 Phase changes to β and α-TCP of HA and GR-HA's.

it seems as though the presence of secondary phases predominate the level of shrinkage.

Since there are no data obtained for porosity and amount of secondary phases below 1200 °C, there is no way of determining whether or not these factors have an affect on the difference in the level of shrinkage seen between these materials below 1200 °C.

It has been reported that the degradation of the HA phase to secondary phases may also influence the strength in the material [2]. The correlation between the strength (Fig. 5) and the presence of these secondary phases (Fig. 4) can be clearly seen. At 1200 and 1250 °C there is an increase in the mean strength of both GR-HA's compared to HA, this is reflected by the amount of β-TCP present in both materials. However, at 1300 and 1350 °C, the results diverge showing a decrease in the mean strength of GR-HA (5) and a sharp increase in strength for GR-HA (2.5). It has been suggested that these phase changes bring about transformation toughening through residual stress, which

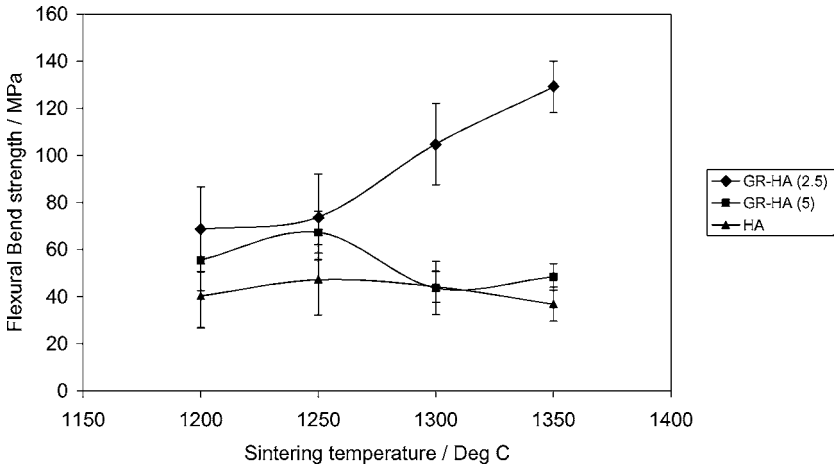

Figure 5 Biaxial flexural strength of HA and GR-HA's.

limits the probability of failure [3]. It is evident in this case that the amount of α-TCP is critical [3].

It is important to consider the affect of porosity on the strength of the material (Fig. 3). GR-HA (5) exhibits an increase in porosity at 1300 and 1350 °C. This also correlates with the drop in strength shown at these temperatures (Fig. 5).

The results suggest that porosity may to some extent influence the level of shrinkage during sintering and the subsequent biaxial flexure strength of the materials, however, the dominating factor that influences these aforementioned properties is attributed mainly to the presence of secondary phases.

References

1. R. H. DOREMUS, *J. Mater. Sci.* **27** (1992) 285.
2. J. C. KNOWLES, S. TALAL and J. D. SANTOS, *Biomaterials* **17** (1996) 1437.
3. G. GEORGIOU and J. C. KNOWLES, *ibid.* **22** (2001) 2811.
4. D. C. TANCRED, B. A. O. McCORMACK and A. J. CARR, *ibid.* **19** (1998) 1735.
5. M. LOPES, F. J. MONTEIRO and J. D. SANTOS, *ibid.* **20** (1999) 2085.
6. L. J. JHA, J. D. SANTOS and J. C. KNOWLES, *J. Biomed. Mater. Res.* **31** (1996) 481.

Received 20 May
and accepted 10 October 2003